On the alignment, integration, and testing of the Raman spectrometer for MMX (RAX)

Martin Pertenais, Conor Ryan, Ute Böttger, Maximilian Buder, Yuchiro Cho, et al.

Martin Pertenais, Conor Ryan, Ute Böttger, Maximilian Buder, Yuchiro Cho, Sven Gutruf, Till Hagelschuer, Heinz-Wilhelm Hübers, Andoni G. Moral, Olga Prieto-Ballesteros, Steve Rockstein, Selene Rodd-Routley, Fernando Rull, Friedrich Schrandt, Susanne Schröder, "On the alignment, integration, and testing of the Raman spectrometer for MMX (RAX)," Proc. SPIE 12180, Space Telescopes and Instrumentation 2022: Optical, Infrared, and Millimeter Wave, 121800F (27 August 2022); doi: 10.1117/12.2626701

SPIE.

Event: SPIE Astronomical Telescopes + Instrumentation, 2022, Montréal, Québec, Canada

On the Alignment, Integration and Testing of the RAman Spectrometer for MMX (RAX)

Martin Pertenais[a], Conor Ryan[a], Ute Böttger[a], Maximilian Buder[a], Yuichiro Cho[b], Sven Gutruf[c], Till Hagelschuer[a], Heinz-Wilhelm Hübers[a], Andoni G. Moral[d], Olga Prieto-Ballesteros[e], Steve Rockstein[a], Selene Rodd-Routley[a], Fernando Rull[f], Friedrich Schrandt[a], and Susanne Schröder[a]

[a]German Aerospace Center (DLR), Institute of Optical Sensor Systems, Rutherfordstr. 2, 12489 Berlin, Germany
[b]Department of Earth and Planetary Science, The University of Tokyo, 7-3-1 Hongo, Bunkyo, Tokyo 113-0033, Japan
[c]Kampf Telescope Optics GmbH (KTO), Alois-Gilg-Weg 7, 81373 Munich, Germany
[d]National Institute for Aerospace Technology (INTA), Ctra. Aljalvir km. 4. 28850 Torrejón de Ardoz, Spain
[e]Centro de Astrobiología (CAB-INTA-CSIC), 28850 Torrejón de Ardoz, Spain
[f]Grupo de Astrobiologia ERICA, Universidad de Valladolid. Av. Francisco Valles, 8. 47152 Valladolid, Spain

ABSTRACT

The Martian Moons eXploration (MMX) mission led by JAXA will conduct remote sensing of both Martian moons Phobos and Deimos and in-situ observations and return samples from Phobos. A small rover will be operating on Phobos' surface and perform scientific measurements, in particular with its Raman Spectrometer for MMX (RAX). The instrument is jointly developed by DLR with partners from Spain (INTA, University of Valladolid) and Japan (JAXA, University of Tokyo). With its more than 20 optical elements (e.g. laser, lenses, mirrors, grating, dichroic beam-splitters, spectral filters), the optical alignment and integration of this very compact Raman spectrometer was one of the biggest challenges of the instrument development at DLR. This article will cover the different steps of alignment with 1) the integration of the lenses in each individual lens group, 2) the alignment and integration of each lens group to build the spectrometer, and 3) the global alignment verification of the end-to-end instrument. The main goal was to integrate the optical elements in RAX's mechanical housing providing maximized scientific performance. This meant for example that the detector's sensitive surface had to be precisely placed at the focal plane surface of the imaging objective to optimize the spectral resolution, but also that the confocality of the laser output (and image on Phobos' surface) with the spectrometer slit had to be very accurately adjusted to optimize the Signal to Noise Ratio of the Raman features. Aligning and integrating a state-of-the art Raman spectrometer in a very compact volume of less than 10x10x10 cm^3 and a mass lower than 1.5 kg was challenging but successful. The different tests performed on the instrument presented here also showed the robustness of the design and demonstrated that RAX can perform excellent scientific measurements on Phobos.

Keywords: AIT, Raman, Optical Alignment, MMX, RAX

1. INTRODUCTION

1.1 RAX Scientific goals

The RAX scientific objectives are following closely from the science objectives of the MMX mission and the MMX rover. The central question of the MMX mission concerns the origin of the martian moons, which could

Further author information: Send correspondence to martin.pertenais@dlr.de

Space Telescopes and Instrumentation 2022: Optical, Infrared, and Millimeter Wave, edited by Laura E. Coyle, Shuji Matsuura, Marshall D. Perrin, Proc. of SPIE Vol. 12180, 121800F · © 2022 SPIE · 0277-786X · doi: 10.1117/12.2626701

have formed for instance from an impact or could be captured. Analysis of the mineral composition of Phobos can help to differentiate between the different hypotheses. Next to directly addressing this scientific question, the MMX rover shall additionally support risk mitigation for the MMX lander with in-situ data. In order to achieve these goals, the RAX instrument should fulfil the following tasks during its mission, where the first one is of highest priority:

- Investigation of the surface mineralogy on Phobos with Raman spectroscopy
- Investigation of surface heterogeneities by measuring at different locations on Phobos
- Potentially supporting the characterisation of the MMX lander landing site
- If possible, support the selection of samples for the return to Earth
- Comparison of RAX scientific measurements with Raman data obtained from the surface of Mars[1]

The primary objective of the RAX instrument is the investigation of the surface mineralogy on Phobos by spectral identification using Raman spectroscopy.[2] RAX is designed to cover the range up to 4000 cm^{-1} with a spectral resolution of <15 cm^{-1} wherein all important Raman features including bonds with hydrogen can be detected. The majority of Raman peaks from minerals is typically seen between 50 cm^{-1} to 1200 cm^{-1}.[3]

1.2 RAX Optical Design Description

The RAX instrument consists of two physically separated units, the RAX Laser Assembly (RLA) and the RAX Spectrometer Module (RSM), which are connected with an optical fiber.[4] The RLA consists of a Raman laser, which is based on a laser unit developed for the ExoMars2022 mission[5] by Instituto Nacional de Tecnica Aerospacial (INTA) and University of Valadolid (UVa). The laser provides an emission wavelength of 532 nm and an optical output power of up to 100 mW. The RSM is the main module of the RAX instrument. It consists of a very compact optical assembly with an actuator for laser auto-focusing jointly developed by DLR and JAXA/University of Toyko (UTo), and a lightweight, space-qualified CMOS detector.[6] In-situ measurements of Raman spectra on Phobos will be realized by autonomously focusing the laser beam, provided by the RLA, onto the ground at a distance of 80 mm from the entrance optics below the rover.

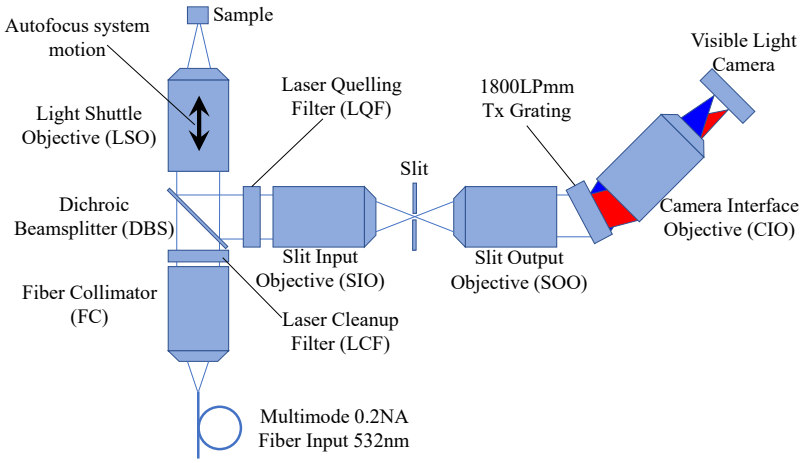

Figure 1. Simplified schematic description of the optical design of RAX, excluding folding mirrors.

As shown in Figure 1, the optical design of RAX RSM is complex and includes several optical sub-systems:

- The **Fiber Collimator (FC)** is a simple two-lens objective collimating the input laser light fed through a multimode fiber from the RLA. A laser clean-up filter (532nm ±1.5nm) is set at the output of this objective to make sure that the Raman excitation light is precisely at 532nm

- The **Dichroic Beam-Splitter (DBS)** transmits the excitation light below 534nm, and reflects the higher wavelengths that are emitted by Phobos' surface
- The **Light Shuttle Objective (LSO)**, as part of the **AutoFocus Sub-system (AFS)**, both focuses the laser light onto Phobos' surface and gathers the Raman scattering to feed the spectrometer. It is a six-lens objective.
- The **Light Preparation Module (LPM)** is composed of a Slit Input Objective (SIO) focusing the collimated beam emerging from the LSO into a Slit, and a Slit Output Objective (SOO) collimating the output of the slit
- This collimated beam is folded, via the grating mirror, towards the grating that disperses the Raman light spectrally
- the **Camera Interface Objective (CIO)**, the most complex optical component being a telecentric seven-lens objective, focuses this spectrum onto the CMOS detector.

1.3 Laboratory Setups

In order to perform the alignment and integration of these optical sub-systems, an Optical Ground Segment Equiment (OGSE) was set up in the laboratory clean-room.

Fig. 2 shows a picture of this setup and identifies the 3 different optical paths available:

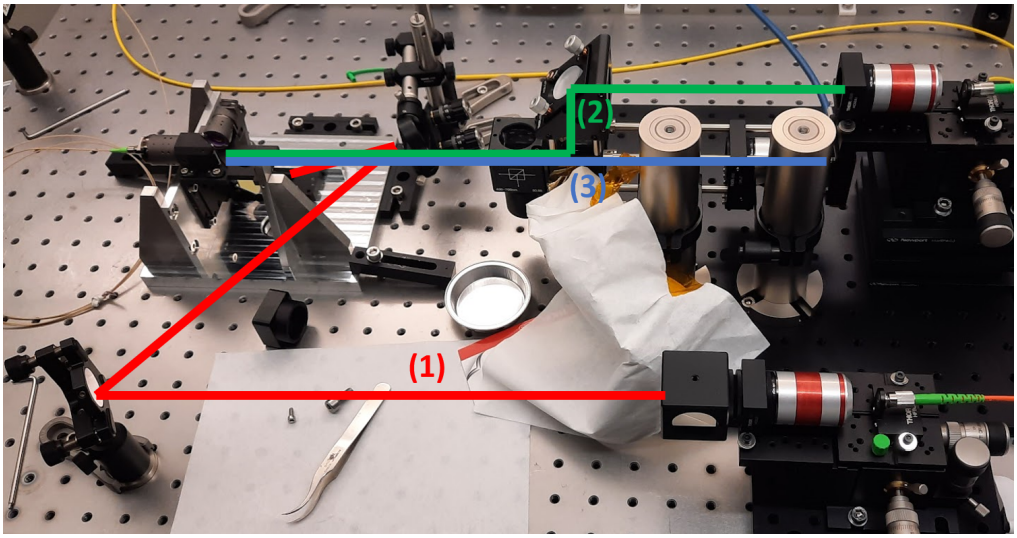

Figure 2. Picture of the OGSE used for most of alignment and integration steps described in this paper.

1. the red optical path labelled (1) uses a periscope-like setup with two folding mirrors allowing the operator to access the optical path of the LPM output, grating and the grating mirror. Collimated or diffused light can be fed into the instrument with this path. It can also be used in the opposite direction, by analysing the light exiting the instrument through this path.
2. the green path labelled (2) is very similar to (1), with the main difference that it is co-aligned with the Fiber Collimator and/or LPM input. A light source can be placed at its source to send light (laser or polychromatic) into the DBS, or a fiber-fed spectrometer can be installed to measure the output spectrum of the DBS.
3. the blue path labelled (3) shares the same optical axis as (2), and has a laboratory camera installed at its end. The cameras detector is confocal to the slit and the fiber tip of RAX.

2. SUB-SYSTEMS ALIGNMENT

2.1 Lens integration

The different optical objectives presented in Sec. 1.2 were individually manufactured, aligned and integrated by the company KTO. The only exception is the AFS, including the LSO, that was developed by University of Tokyo and JAXA.

Each objective was individually integrated and aligned. To do so, each lens was first integrated in its own mechanical assembly and glued to it. These opto-mechanical sub-assemblies, visible on Fig. 3 for all 7 lenses of the CIO, could then be installed in the right chosen sequence inside the main objective barrel.

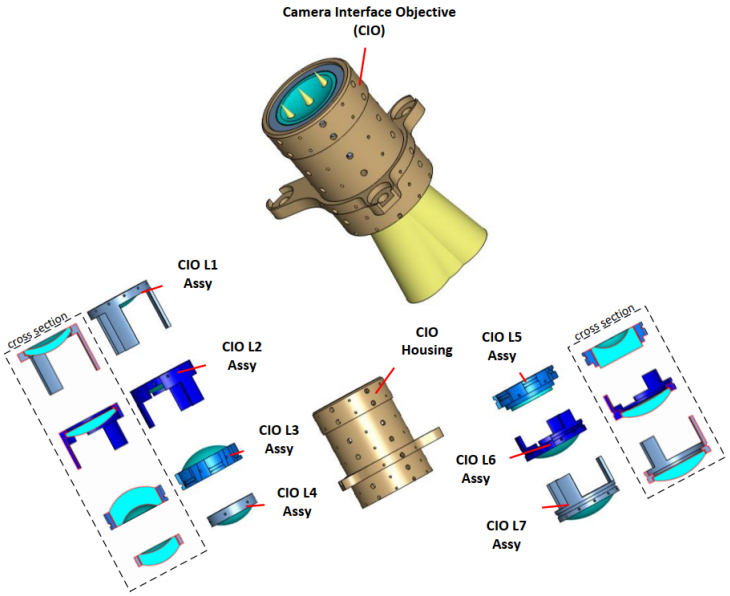

Figure 3. Exploded schematic view of the CIO opto-mechanical parts.

The transmitted wavefront error was measured after integration of each lens assembly, allowing us to adjust the lens positioning to its optimal position in the mechanical housing. This was achieved by precise alignment screws that were placed through the housing, as seen on Fig. 4. Using these screws on every lens sub-assembly, the centering and angular position of the lens relative to each other and relative to the mechanical housing could be controlled with a live wavefront error measurement though the objective. A comparison with the as-built optical design model, created with an optical design CAD software using the measurement of the lenses positions, could be performed to eventually place all the lenses in their optimal position. When this is reached and the performance of the objective verified, all lenses sub-assemblies could be glued to the mechanical housing in order to secure their position.

2.2 Fiber Collimator

The first step in the sub-system alignment procedure is to perform a preliminary co-alignment between the fiber input delivering the laser light into the RSM, and the FC. The interface between the fiber and the FC is a mini-AVIM ® connector. This interface can be translated in the X/Y image plane of the FC (to bring the fiber output on the optical axis of the FC) and translated along this optical axis by a rotating barrel inside the FC.

The FC was initially visually collimated and pre-aligned in the X/Y direction using a pinhole centred in front of the output collimated beam. Using a Shack-Hartmann sensor, the FC Barrel was rotated inside the FC to modify the focus position of the fiber output with respect to the optics and minimize the defocus error in the wavefront. The final result, after tightening of the retaining ring is a Zernike defocus coefficient smaller than 0.005λ at 532 nm. The mini-AVIM ® connector X-Y position was then adjusted by hand to minimize the

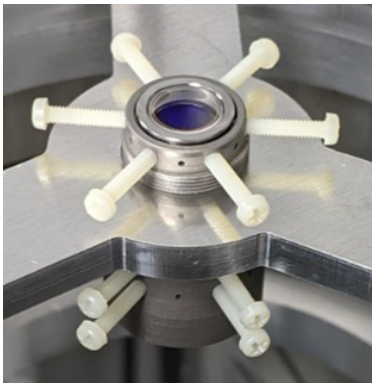

Figure 4. Picture of the Slit Input Objective during its lens alignment.

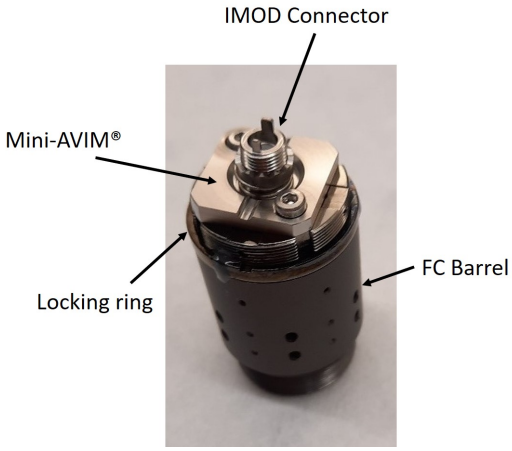

Figure 5. Picture of the Fiber Collimator with its mini-AVIM ® interface on the IMOD connector interfacing with the laser fiber (not shown).

global wavefront error by placing the fiber output tip as close to the optical axis as possible. The final result obtained is a Peak-to-Valley Wavefront Error (WFE) of 0.21λ and 0.05λ RMS. This is twice as good as the result obtained with RAX development model. This procedure was repeated after integration of the FC into the casing, see Sect. 3.

2.3 Dichroic Beam-Splitter Assembly

The FC was prepared with the clean-up filter already glued into place at its output. The filter limits transmission through the FC to (532 $\pm$1.5) nm, which prevents its use in any optical system to test the DBS spectral cut-off at 534.2 nm. The FC was therefore removed from the GSE and the dichroic illuminated from the other side, enabling the direct measurement of the transmission spectrum of the dichroic. This was done using a collimated white beam from a polychromatic LED and a standard laboratory visible spectrometer. Fig. 6 shows the measured transmission spectrum with a mid-point of the transmission drop at 534.3 nm. Considering that the requirement is to be at (534.2 $\pm$)0.8 nm, the result is acceptable.

After the LPM integration and confocality alignment (see Sect. 3), the reflection spectrum of the DBS could also be measured and confirmed the previous transmission measured. This was done by placing a fiber-fed spectrometer on the green path (2) of Fig: 2 and illuminating the DBS via the red path (3) with a white LED.

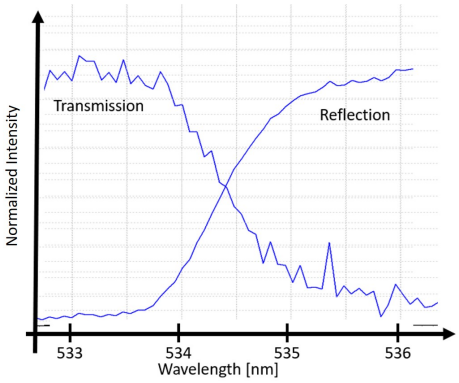

Figure 6. Measured transmission and reflection spectra of the DBS.

2.4 Light Preparation Module Assembly

2.4.1 Collimation verification

The Light Preparation Module (LPM) was delivered with both Slit Input Objective (SIO) and the Slit Output Objective (SOO) pre-aligned with the slit in-between. The first step was therefore to verify the collimation performance of both the SIO and the SOO. The LPM is installed on the Optical Monolith as well as the already aligned FC and DBS Assembly and the lower base grating mirror to help access the SOO, as shown in Fig. 7. The optical monolith is a mechanical piece, part of the final flight instrument, that holds in place most of the optical sub-systems in a stable relative positions with each others.

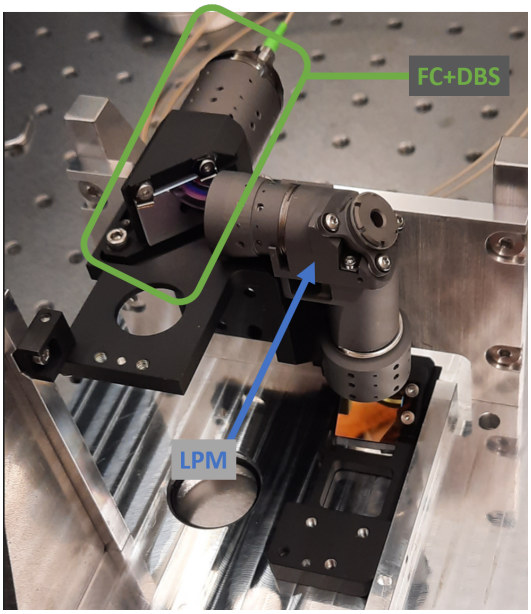

Figure 7. Setup used for the LPM assembly alignment. Both the FC and DBS (highlighted in green) and the LPM are installed on the so-called optical monolith in their relative flight configuration.

The SIO's collimation is verified by illuminating the slit (via the grating mirror and the SOO) with a 633 nm laser beam. The measured wavefront error (WFE) of the SIO is 0.17 λ PV with a defocus Zernike coefficient of 0.001λ. This is compatible with the WFE measured after the objective integration with 0.34 λ PV, measured in double pass.

The other way around, the red laser is then input into the SIO via the dichroic beam splitter (using the green path (2) of Fig 2). However, as the image of the laser beam on the slit is smaller than the slit, the wavefront error measured as output of the SOO is therefore the combination of both the SIO and the SOO. The WFE measurement was dependent on the position and orientation of the Shack-Hartmann sensor with a PV value of the WFE changing between 0.3 and 0.4 λ PV. It is also in line with KTO's measurement and therefore confirms the quality of LPM.

2.4.2 Laser-Slit Confocality Alignment

With the collimation performance of the LPM being verified in both directions and compliant with the requirements, the confocality alignment of the excitation laser output with the slit can be performed. This is critical since it ensures that the Raman signal, emitted from the position of the laser spot on the surface of Phobos, passes correctly through the slit to be analysed by the spectrometer. This confocality alignment is performed by fine-tuning the lateral X/Y position of the laser fiber output in the focal plane of the FC.

Using the OGSE setup presented in Sect. 1.3, a laboratory camera (at the end of the blue path (3) of Fig. 2) is used to image simultaneously the output of the fiber (laser) through the DBS and the FC, as well as the slit. To illuminate the slit, diffuse light was introduced into the SOO via the grating mirror (visible in Fig. 7), fully illuminating the slit from behind.

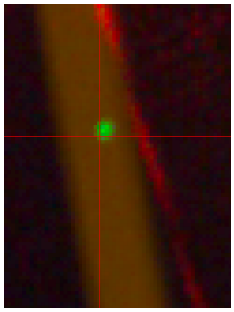

Figure 8. Achieved confocality of the excitation laser output and the slit.

Fig. 8, shows the achieved confocality, with both the slit and the laser fiber output imaged on the laboratory camera.

2.5 Camera Interface Objective Assembly

The alignment and focusing of the Camera Interface Objective (CIO) onto the detector, see Fig. 9, is independent from the previous steps, and could be performed in parallel. The cutting-edge method described in Pertenais et al. [7] enabled a very quick and efficient alignment of the CIO using a Diffractive Optical Element (DOE) to create a pattern of collimated beams across the full camera field of view.

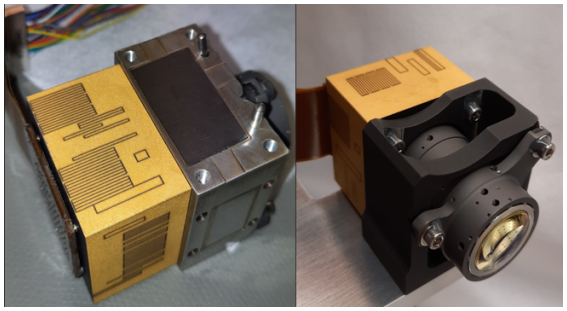

Figure 9. Picture of the Camera Interface Objective attached to the 3D+ CMOS flight detector.

The pattern of collimated beams produced by the DOE is imaged on the detector by the CIO. An analysis script is computing for each of these points the Ensquared Energy Fraction of the PSF inside 3x3 pixels. The higher this number, the more in focus the CIO is for the wavelength used in the measurement. The longitudinal chromatism of the CIO being corrected by design, it is sufficient to work with monochromatic light. To be able to assess different relative focus positions between the CIO and the detector, the incoming beam illuminating the DOE was defocused in a controlled way. Based on the known defocus imposed to the beam (thanks to precise translation stage Vernier screws), the equivalent physical defocus could be computed and corresponding shims implemented at the mechanical interface between the detector and the objective. Fig. 10 shows the result of the first iteration loop, showing a strong variation of the ensquared energy as a function of the defocus. An equivalent defocus of 100 to 125 µm was computed based on these measurements. This 100 to 125 µm defocus was in the negative direction (detector too far away from the objective) and we therefore had to mill down 150µm of the hemispherical washers supporting the objective on the detector mechanical interface.

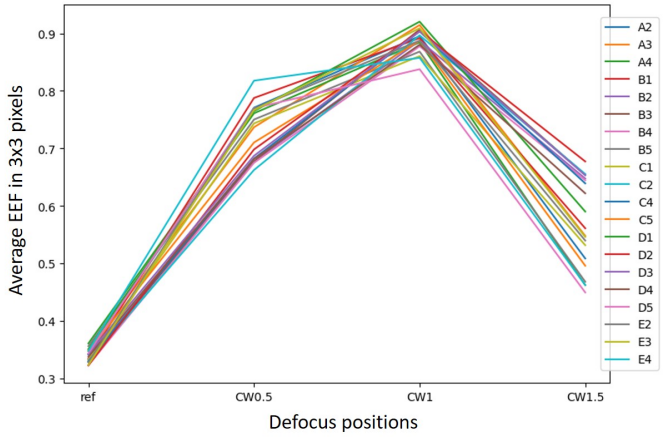

Figure 10. Plot of the merit function used to determine the best focus position of the CIO wrt the detector, for different positions in the field of view.[7]

The measurement was then repeated with the shortened mechanical interface. The ensquared energy fraction showed an excellent quality ($> 90\%$ in 3x3 pixels) with a collimated beam and proved to be very stable with small defocused beam in both directions. We could therefore conclude that we were on the plateau of best focus. The details of this innovative measurement method is described in Ref. 7.

Another setup was developed at DLR to be able to verify this alignment with a more conservative measurement technique. A spectrum simulation station was build, creating a spectrum with a duplicate of the RAX Grating. In this way, the same wavelength range and the same geometrical characteristics as RAX are simulated. Only the spectral resolution is different as a different slit size was used. Similarly to the DOE setup, this spectrum simulation station provides the capability to control the defocus of the incoming beam thanks to the fine controlled translation of the objective imaging the slit. Spectra were acquired in the full wavelength range of RAX for several controlled defocused incoming beams illuminating the CIO. By computing the spectral resolution achieved for the different positions, the best focus position could be estimated. Using this setup, a value of 100µm $\pm$50µm was computed, and therefore confirmed the measurement with DOE.

Finally, some spectra were acquired again after the shorter mechanical interface was implemented, to confirm the positive result of this action. Fig. 11 shows a extract of some spectral lines observed with different beam collimation. This confirms that the best focus position is now reached with the sharper lines observed with a perfect collimated beam.

2.6 Grating and Grating Mirror Assembly

In order to correctly align and integrate the grating mirror and the grating itself (shown in Fig. 12), all pre-aligned sub-assemblies are installed in the Mechanical Ground Segment Equipment (MGSE) jig: the FC is put

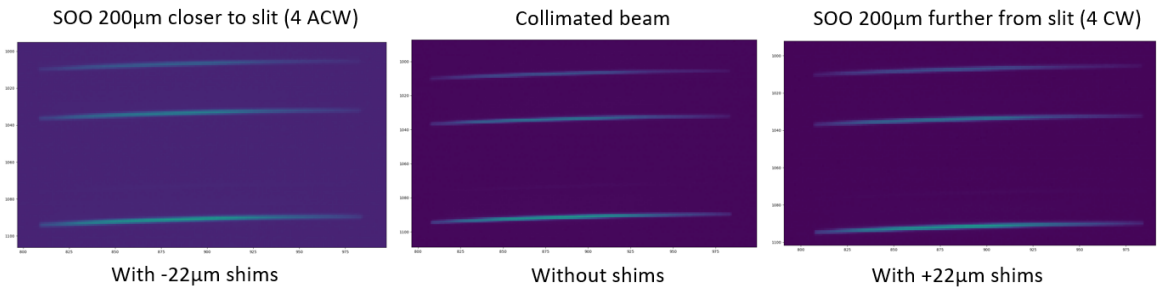

Figure 11. Example of spectral lines observed with different beam collimation, confirming the final focusing of the CIO on the detector.

in place attached to the DBS assembly, the Light Module Preparation is screwed to the jig and finally the CIO is put in place with the detector.

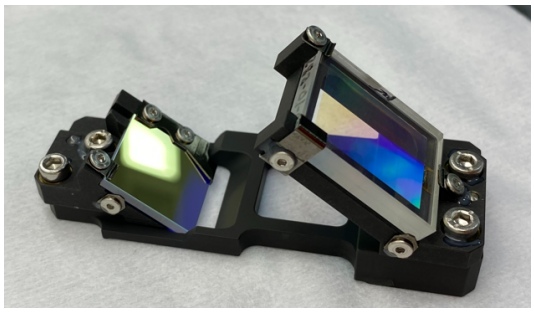

Figure 12. Picture of the so-called lower base assembly, holding a folding mirror and the grating of RAX.

This setup allowed us to acquire a spectrum with the FM detector of any lamp put in front of the DBS. Fig. 13 shows an example with a laboratory Neon lamp.

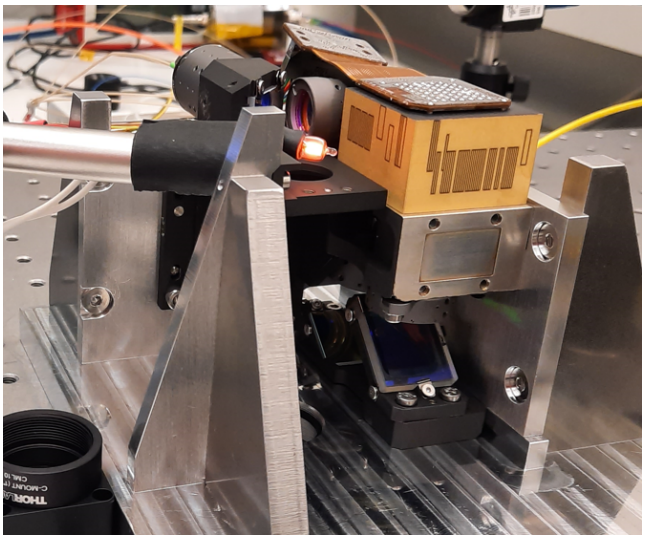

Figure 13. Measurement setup using a Neon lamp as excitation to measure a spectrum with the almost end-to-end RSM chain.

Using the detector in video mode, the grating was rotated around its dowel pin to align the spectral dispersion axis as well as possible with pixel columns of the detector. The figure below shows two examples of spectra acquired. The right spectrum corresponds to one of the extreme position possible considering mechanical constraints. It is therefore the final position chosen.

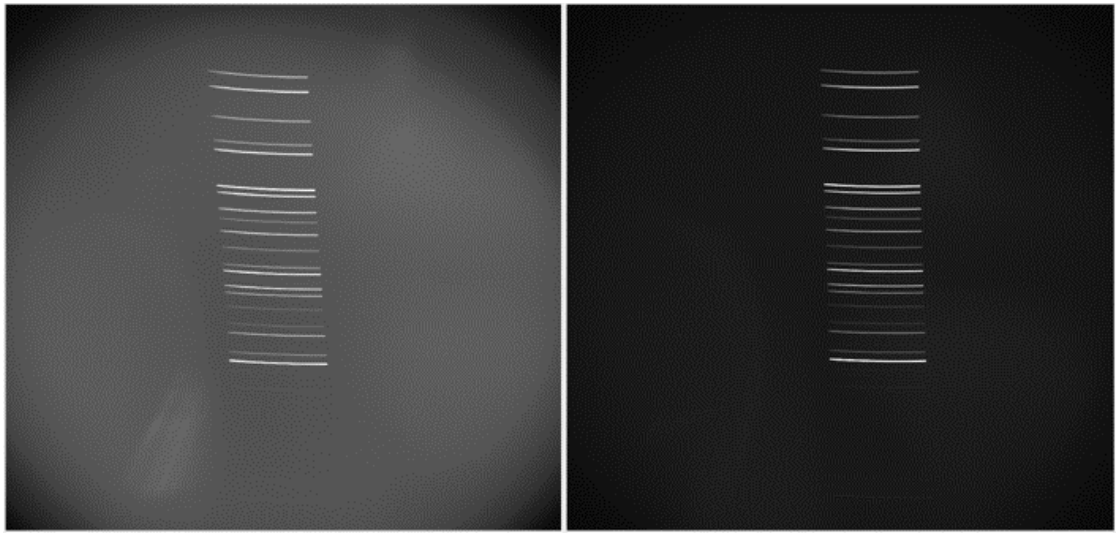

Figure 14. Images of Neon spectra measured with the FM detector with the 2 extreme different grating positions.

With the spectrum orientation aligned to the detector, the next step was to optimize the wavelength range illuminating the detector. As a reminder, the requirement is to detect the excitation laser line at 532 nm for reference of the Raman spectrum and observe the spectrum to at least 680 nm.

In the measured spectrum, shown in Fig.14, the laser line is unfortunately not visible (expected to be at the lower edge of the image. To retrieve it, the LPM (pre-aligned in Sec. 2) was tilted around the spectral direction as much as possible to estimate the achievable impact on the spectral range imaged on the detector. After a couple of iteration, shims of 300 µm were introduced and the LPM fixed in this new position. As a result, the spectrum shifted up as expected to bring the laser line inside the CIO and detector field of view. It was also verified that the rotation of the LPM around that particular axis had no impact on the spectrum orientation on the detector.

2.7 Phobos Mirror

The goal of this final step before integration of the sub-systems in the casing is to set the alignment of the Phobos mirror on the optical monolith as accurately as possible prior to installation into the mechanical casing. Once installed in the casing, the Phobos mirror is no longer accessible.

As shown in Fig. 15, the setup used to perform this alignment is the same as previously, with all the sub-systems aligned and installed in their relative flight configuration on the optical monolith. Two pinholes of different sizes are placed in the two available apertures after the Phobos mirror (marked with a green star in the Fig. 15) and a laboratory camera underneath the lowest one.

After a sequential step by step co-alignment of both pinholes, the camera and the laser beam coming out of the FC and reflected by the DBS, the off-axis angle of the projected beam by the Phobos mirror can be evaluated, to a value of 6.4mrad. Considering the mirror length and the projection distance, this tilt angle would correspond to shims below the Phobos mirror of 57µm. With fitting shims available only in steps of 50µm, two single 50µm shims were introduced on the correct side below the two screws supporting the Phobos mirror. The final measurement shows a residual tilt angle of around 1.5 mrad, which is an excellent value to conclude the sub-system integration activities on.

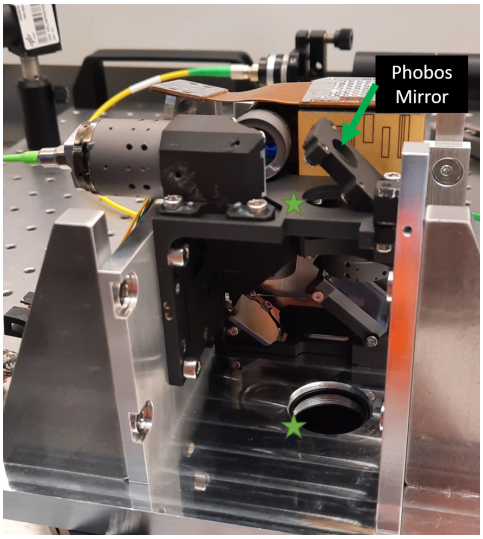

Figure 15. Test setup for the Phobos mirror alignment, using pinholes (not visible in the Figure) in both apertures marked with a green star.

3. INSTRUMENT INTEGRATION

With completion of all steps presented in Sec. 2, the optical sub-systems are ready to be integrated into the RSM Casing.

The biggest hurdle to this installation is that the FC must be removed to allow installation of the sub-assembly in RAX and reinstalled afterwards, an action that may tilt the FC's output beam and thus render the input fiber tip non-confocal with the Slit. If so, the x-position of the FC's mini-AVIM connector must be modified to correct this situation, in a way that does not disturb the FC's collimation. Furthermore, the grating/grating bracket must be removed and replaced in order to assemble the optical monolith and CIO assemblies.

3.1 Mechanical Integration in the Casing

In order to be able to insert the sub-assemblies in the casing, the FC must first be removed. It is therefore unscrewed after noting its rotational position inside its holder. The lower optics assembly (without the grating!) can be directly integrated into the casing and fixed. The detector assembly can then be integrated thanks to its 2 dowel pins, simultaneously with the Optical Monolith. The FC can then be put back in place, as close as possible to its initial rotational position. Before being able to check that the sub-assemblies are at their right position by acquiring a Neon spectrum, the grating has to be installed back on the lower optics assembly.

A Neon spectrum was then acquired by holding the Neon lamp close to the Phobos mirror. This measurement confirmed that the spectrum lies in the same position on the detector as the reference spectrum acquired in the MGSE jig in Sec. 2.6. This validates the integration of the sub-assemblies in the mechanical housing.

3.2 Confocality Fine-tuning

As the Fiber Collimator had to be removed and re-installed, a final confocality check between the laser output and the slit was performed. In order to repeat this measurement already performed before integration, a laboratory camera with a focusing objective was inserted in front the entrance window of RAX, see Fig. 18. By turning on the laser at the focal plane of the FC and illuminating the slit from below through the grating mirror, both laser and slit could be observed simultaneously on the laboratory camera.

As shown in Fig. 18, the laser was initially well centered along the slit but close to the edge of the slit across the slit. To correct for this, the 2 retaining screws of the IMOD connector at the focal plane of the FC were

Figure 16. Pictures of the different optical sub-assemblies now integrated into the FM mechanical housing of RAX RSM with its KeplaCoat blackening inside[8] and Alodine on the external surfaces.

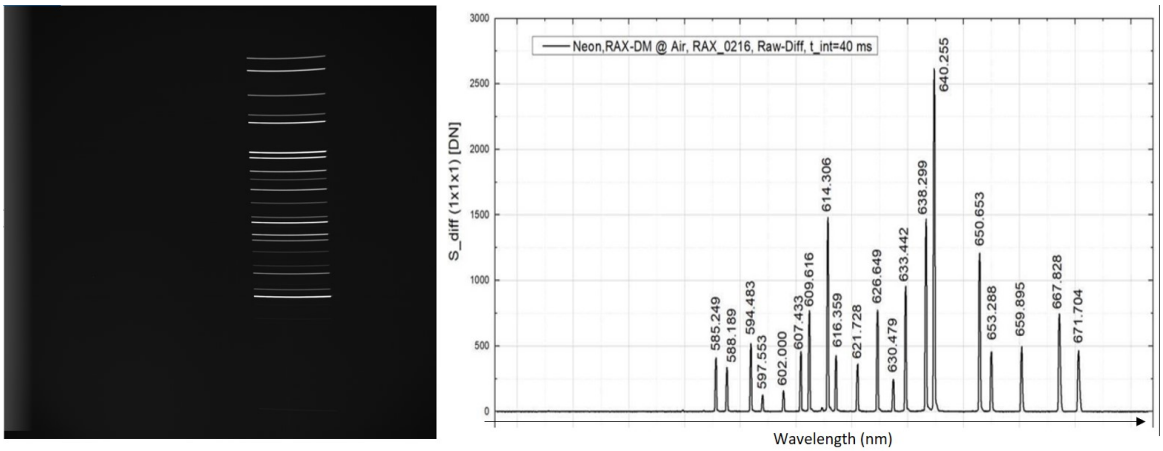

Figure 17. Neon Spectrum acquired with RAX FM, with only the AFS missing in the chain.

carefully loosed and the connector slightly moved around to bring the laser as close as possible to the center of the slit, as shown on the right-hand side of the figure.

Finally, as the position of the laser output has been modified on the focal plane of the FC, its collimation quality had to be verified. The WFE measured is as follows: 0.1λ PV and 0.022λ RMS. This is actually better than the initial value measured in Sec. 2. However, the Zernike defocus coefficient went up from 0.005 to 0.015λ. The was accepted as the defocus is still within the requirement and less critical than the confocality.

3.3 Auto-Focus System Installation

The AFS was delivered in a pre-aligned and verified status. The only step necessary (after the successful incoming inspection) is to mechanically install it into the RSM Casing. It is oriented and fixed with 2 dowel pins and 4 screws on a planar interface.

4. OPTICAL TESTING

In order to verify the proper alignment between the optical axis of the AFS and its mechanical integration, a Raman spectrum was acquired from a test target.

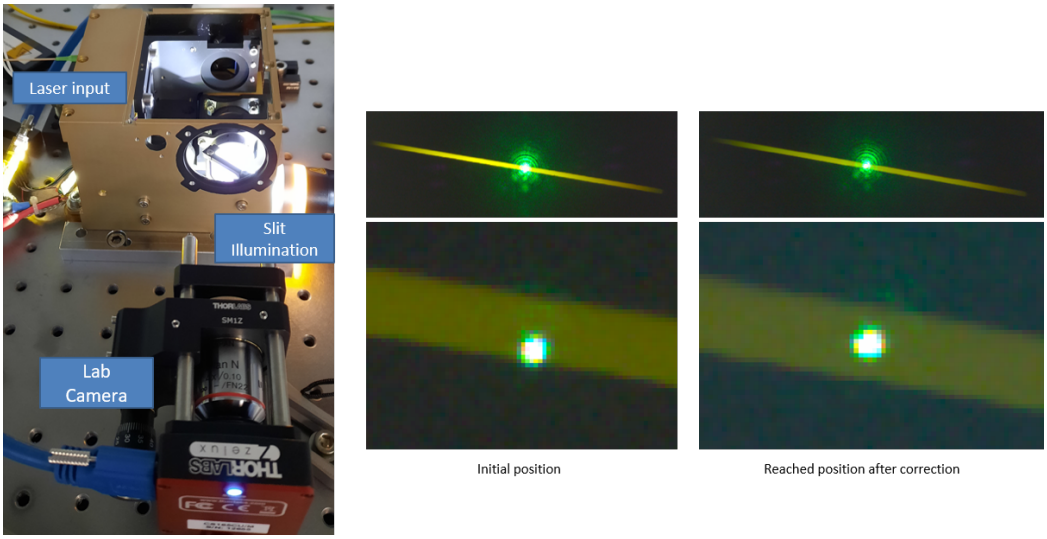

Figure 18. Setup used with the integrated RAX FM to verify and correct the Laser-Slit confocality. Before/After performed is shown on the right-hand side of the figure.

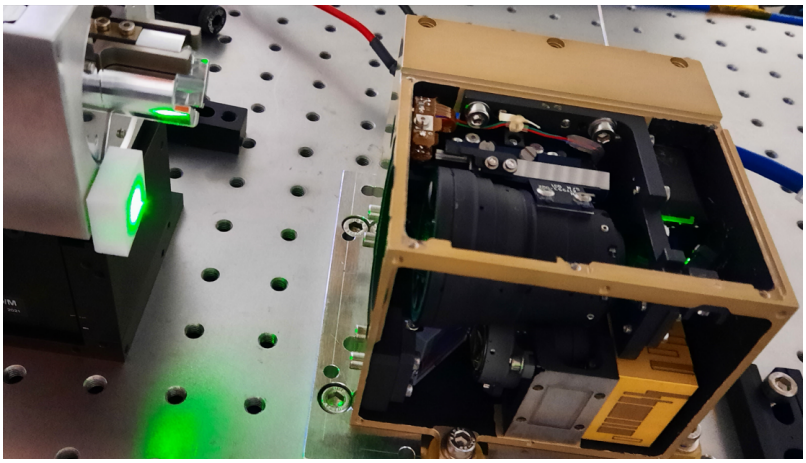

Figure 19. Picture of the first Raman measurement taken after integration of all optical sub-systems into the mechanical housing. The laboratory laser is shoot onto the test target that produces a reference Raman spectrum.

Fig. 19 shows the test configuration with the laboratory laser beam being focused by the LSO inside the AFS. This test allowed us to verify that the beam was coming out of the AFS with the correct angle and well-focused at the expected position.

An image of with the first Raman spectrum acquired with the RSM FM in the laboratory is presented in Fig. 20. The typical Raman features of Ertalye, material of the test target used in this setup, can be seen, in particular the most dominant lines at 1615 cm^{-1} and 1726 cm^{-1}. With this image of a spectrum, the whole alignment and integration process is validated. The spectrum indeed shows compliance to the spectral range observed, the spectral resolution, and the Signal to Noise Ratio obtained along the spectrum.

On the lower part of the image, the laser line is to be seen marking the reference wavelength for the Raman spectrum spreading up to 690 nm (against 680 nm required). A small smile effect is visible with the spectral line behind slightly distorted in the spatial direction, as expected by the design. As the incoming beam was tilted off-axis to align the the pixel columns and the spectral dispersion axis in Sec. 2.6, the spectrum doesn't travel through the CIO along its optical axis and the radial geometric distortion of the objective is visible creating a slightly bent spectrum.

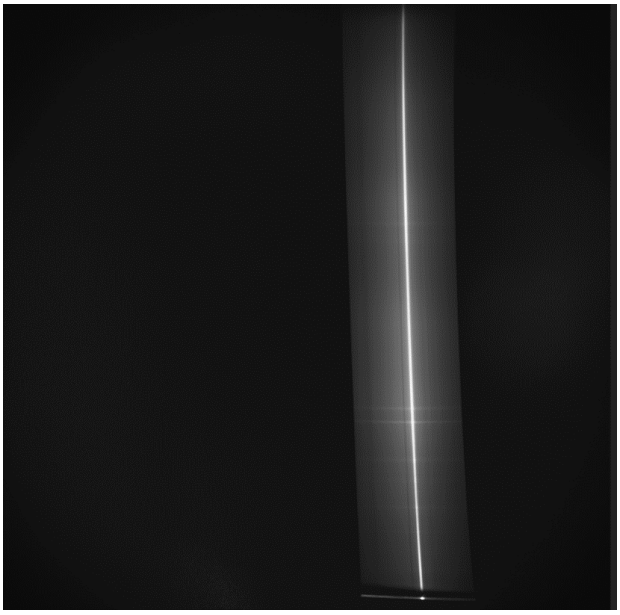

Figure 20. First Image of a Raman spectrum acquired with the flight spectrometer module of RAX.

5. CONCLUSION AND OUTCOME

The optical integration and alignment of RAX Spectrometer Module as been a challenging and critical phase of the instrument development. The individual alignment of the lenses inside the objectives has been the first step in this process. Thanks to accurate relative positioning control of each lens inside the objective mechanical housing and live wavefront error measurement, each objective could be integrated and aligned in a couple of days of work. More importantly and despite the extremely small size of the lenses (<1cm diameter), each objective could be integrated and aligned very accurately and achieving the required optical performance.

Using these pre-aligned objectives, the next step of the integration process was to relatively align them with respect to each other in their flight configuration. Due to the complex optical beam path filling the full volume of RAX RSM mechanical housing in three dimensions, this was performed on a dedication MGSE in the laboratory and not directly in the flight mechanical housing. When this was fully performed and the relative position of each objective fixed and secured on the common so-called optical monolith supporting them mechanically, the final integration into the mechanical housing could be performed. Finally, the verification of the performance and especially the fine-tuning of confocality between the spectrometer slit and the laser output was performed in the flight configuration. The first Raman spectrum acquired confirmed the successful process of alignment and integration of the spectrometer.

REFERENCES

[1] Rull, F., Maurice, S., Hutchinson, I., Moral, A., Perez, C., Diaz, C., Colombo, M., Belenguer, T., Lopez-Reyes, G., Sansano, A., Forni, O., Parot, Y., Striebig, N., Woodward, S., Howe, C., Tarcea, N., Rodriguez, P., Seoane, L., Santiago, A., Rodriguez-Prieto, J. A., Medina, J., Gallego, P., Canchal, R., Santamaría, P., Ramos, G., Vago, J. L., and RLS Team, "The Raman Laser Spectrometer for the ExoMars Rover Mission to Mars," *Astrobiology* **17**, 627–654 (July 2017).

[2] Michel, P., Ulamec, S., Böttger, U., Grott, M., Murdoch, N., Vernazza, P., Sunday, C., Zhang, Y., Valette, R., Castellani, R., Biele, J., Tardivel, S., Groussin, O., Jorda, L., Knollenberg, J., Grundmann, J. T., Arrat, D., Pont, G., Mary, S., Grebenstein, M., Miyamoto, H., Nakamura, T., Wada, K., Yoshikawa, K., and Kuramoto, K., "The MMX rover: performing in situ surface investigations on Phobos," *Earth Planets and Space* **74** (Jan. 2022).

[3] Cho, Y., Böttger, U., Rull, F., Hübers, H.-W., Belenguer, T., Börner, A., Buder, M., Bunduki, Y., Dietz, E., Hagelschuer, T., Kameda, S., Kopp, E., Lieder, M., Lopez-Reyes, G., Moral Inza, A. G., Mori, S., Ogura, J. A., Paproth, C., Perez Canora, C., Pertenais, M., Peter, G., Prieto-Ballesteros, O., Rockstein, S., Rodd-Routley, S., Rodriguez Perez, P., Ryan, C., Santamaria, P., Säuberlich, T., Schrandt, F., Schröder, S., Stangarone, C., Ulamec, S., Usui, T., Weber, I., Westerdorff, K., and Yumoto, K., "In situ science on Phobos with the Raman spectrometer for MMX (RAX): preliminary design and feasibility of Raman measurements," *Earth, Planets and Space* **73**, 232 (Dec. 2021).

[4] Hagelschuer, T., Belenguer, T., Böttger, U., Buder, M., Cho, Y., Dietz, E., Gensch, M., Hanke, F., Hübers, H.-W., Kameda, S., Kopp, E., Kubitza, S., Moral, A., Paproth, C., Pertenais, M., Peter, G., Rammelkamp, K., Rodriguez, P., Rull, F., Ryan, C., Säuberlich, T., Schrandt, F., Schröder, S., Ulamec, S., Usui, T., and Vance, R., "The raman spectrometer onboard the mmx rover for phobos," in [*70th International Astronautical Congress (IAC)*], *70th International Astronautical Congress, IAC 2019* (Oktober 2019).

[5] Benito, M., Rodriguez, P., Rodriguez, J., and Moral, A., "Flight laser module characterization for the ExoMars Raman Laser Spectrometer under a potential depressurization," in [*International Conference on Space Optics — ICSO 2020*], Cugny, B., Sodnik, Z., and Karafolas, N., eds., **11852**, 2799 – 2807, International Society for Optics and Photonics, SPIE (2021).

[6] Ryan, C., Ulamec, S., Kameda, S., Rull, F., Schröder, S., Hübers, H.-W., Usui, T., Böttger, U., Belenguer Davila, T., Moral Inza, A. G., Gensch, M., Buder, M., Hagelschuer, T., Kopp, E., Cho, Y., Pérez, C., Peter, G., Rodriguez, P., Routley, S., Säuberlich, T., Schrandt, F., Dietz, E., and Yumoto, K., "RAX - A compact instrument for Raman Spectroscopy aboard the Phobos rover of the MMX mission," in [*43rd COSPAR Scientific Assembly. Held 28 January - 4 February*], **43**, 211 (Jan. 2021).

[7] Pertenais, M., Ryan, C., Griessbach, D., and Routley, S., "Usage of a Diffractive Optical Element (DOE) for best focal plane estimation of a camera during the integration process," *Proc. SPIE* **XX**, XX (2022).

[8] Ryan, C., XXX, S., and Böttger, U., "Measurements of black surface treatments for straylight and fluorescence suppression in the RAman Spectrometer for MMX (RAX)," *Proc. SPIE* **XX**, XX (2022).